J Mater Sci (2013) 48:612–624
DOI 10.1007/s10853-012-6938-5

REVIEW

Zinc oxide nanostructures: from growth to application

Jorge L. Gomez · Onur Tigli

Received: 9 April 2012 / Accepted: 5 October 2012 / Published online: 9 November 2012

Abstract Zinc oxide's (ZnO) physical and chemical properties make it a viable and extremely attractive compound to use in a variety of nanotechnology applications. Some of these applications include biomedical, energy, sensors, and optics. As the research in ZnO nanostructures continue to grow, it has inspired a whole host of new innovative applications. Complementing its unique chemical qualities, it also has a simple crystal-growth technology and offers significantly lower fabrication costs when compared to other semiconductors used in nanotechnology. Several processes have been developed in order to synthesize high quality ZnO nanostructures—specifically in the case of nanowires. Here we offer a comprehensive review on the growth methods currently employed in research, industry, and academia to understand what protocols are available to meet specific needs in nanotechnology. Methods examined include: the vapor–liquid–solid, physical vapor deposition, chemical vapor deposition, metal–organic chemical vapor deposition, and the hydrothermal-based chemical approach. Each of these methods is discussed and their strengths and weaknesses are analyzed with objective comparison metrics. In addition, we study the current state-of-the-art applications employing ZnO nanostructures at their core. A historical perspective on the evolution of the field and the accompanying literature are also presented.

J. L. Gomez (✉) · O. Tigli
Electrical and Computer Engineering, University of Miami, Coral Gables, FL, USA
e-mail: j.l.gomez@umiami.edu

O. Tigli
e-mail: tigli@miami.edu

O. Tigli
Department of Pathology, Miller School of Medicine, University of Miami, Coral Gables, FL, USA

O. Tigli
Dr. John T. Macdonald Foundation Biomedical Nanotechnology Institute at University of Miami, Coral Gables, FL, USA

Introduction

Zinc oxide has been a prevalent topic in semiconductor research for more than 65 years, with mentions in publications dating as far back as 1945 [1]. It went through episodes of increased attention during the 1950s and 1970s in topics of growth, doping, transport, band-structure, and luminescence. Still, this interest faded because of difficulty in doping both n- and p-type causing attention to shift to compounds in the III–V class due to their reduced dimensions [2].

Zinc oxide's popularity increased again during the 2000s due to its potential for epitaxial layer growth, quantum wells, and nanostructures. Currently, a large focus in ZnO has shifted toward biosensing and optoelectronic applications utilizing nanostructures. In particular, this past decade showed a spike in the number of ZnO nanostructure publications—specifically ZnO nanowires. Figure 1 presents a histogram illustrating the number of ZnO nanowires and nanostructures publications since 2000. As demonstrated by this data, the greatest increase in publications occurred in the mid 2000's and has recently begun to lose its momentum. This is not to say that interest in nanostructure growth or nanotechnology has started to subside but rather an interest in other compounds in nanotechnology applications has begun to burgeon. Some worth mentioning include carbon nanotubes and graphene [3–8]. In 2010, Andre Geim and Konstantin Novoselov were awarded the Noble Prize in Physics "for groundbreaking

experiments regarding 2D material graphene." This attracted much interest in carbon-based compounds which affected ZnO and other materials used in nanostructure growth. To illustrate this point, the number of publications regarding graphene from 1978 to 2008 was 158 while 2008 to the present is 3,964 (Source: Science Citation Index Web of Science, ISI Web of Knowledge with the term "graphene" and "nano" in the title; search date March 23, 2012). But despite this current trend in the general field of nanostructures, Zinc oxide is still one of the most studied chemical compounds in nanotechnology. In part due to the vast amount of unique properties and potential application of its nanostructures that can be synthesized with great control and precision. However, popularity in ZnO nanowires is much larger than that of ZnO nanostructures because there are more applications involving 0D and 1D nanostructures than that of 2D and 3D nanostructures.

In order to exploit these applications and obtain a comprehensive understanding of the state-of-the-art in ZnO nanostructures, it is important to examine fabrication methods currently employed in research, industry, and academia. Therefore, five major growth methods are examined in this review: vapor–liquid–solid (VLS), physical vapor deposition (PVD), chemical vapor deposition (CVD), metal–organic chemical vapor deposition (MOCVD), and the hydrothermal-based chemical method. First, we will present a brief overview of ZnO properties. Then we will introduce these five major growth methods that are currently in use for the synthesis of ZnO nanostructures with a large focus on ZnO nanowires. Their respective strengths and drawbacks will be examined. Following this, we will present the most prominent applications utilizing some form of ZnO nanostructures as their core element. Finally, we will conclude with a future outlook summarizing the potential research directions and developing interest relating to ZnO nanostructures.

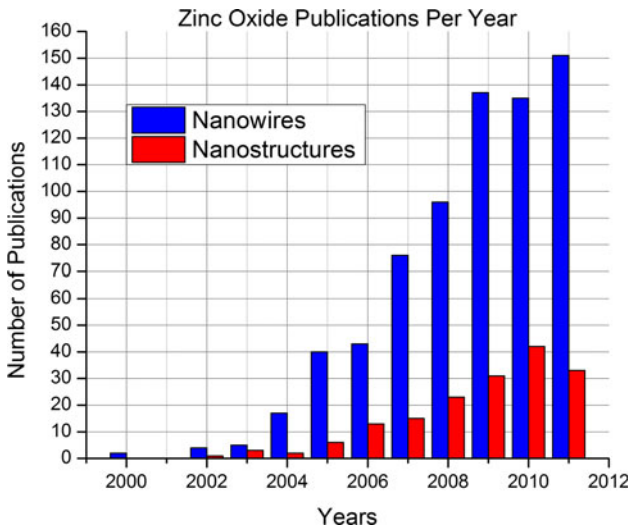

Fig. 1 Histogram of the number of ZnO publication with the term "zinc oxide" and "nanowire" or "zinc oxide" and "nanostructure" in the title. *Source* Science citation index (Web of Science), ISI Web of Knowledge; search date March 23, 2011

Properties

The polar surface of ZnO is very stable and has been used to induce the formation of many different nanostructures such as nanowires, nanorods, nanosprings, nanorings, nanobelts, nanotubes, and nanoflowers [9–18]. This vast morphology along with its wide indirect band gap of 3.37 eV at 25 °C and high excitation binding energy of 60 meV makes it a promising photonic material. ZnO is also tetragonally coordinated so that the center of the positive charges overlaps with that of the negative charges. This means that when an external force is applied, the distortion of the tetrahedron results in a dipole moment, which gives rise to its piezoelectric properties [19].

As a result of ZnO's fast electron transfer kinetics, high isoelectric point (IEP), and biocompatibility, it has displayed potential for biosensing applications. ZnO is a better substitute compared to other chemical compounds used in biosensing such as indium oxide (In_2O_3), which has only a band gap of 2.9 eV. This is because a greater band gap allows for higher breakdown voltage and an ability to sustain large electric fields [20]. Another key quality of ZnO is its IEP of 9.5. Compared to silicon dioxide (SiO_2), whose IEP ranges from 1.7 to 3.5, ZnO's superior IEP allows for the absorption of proteins by electrostatic interaction [21]. Biocompatibility is another important characteristic for biosensors due to in vivo applications. Furthering these advantages, in similar application ZnO has displayed nontoxicity, chemical stability, and electrochemical activity [22].

Other promising applications for ZnO nanostructures are in the optoelectronics field. Some include light emitting diodes (LED) and laser diodes (LD) between the green and the near ultra violet range [23]. In particular, ZnO nanowires' aspect ratio, length to diameter, and surface ratio are higher than those of the bulk or thin-film photodetectors and provide a strong photoresponse. This makes them ideal as a 1D photodetector [24]. Also, ZnO's transparency to visible light promises to replace transparent conductive indium tin oxide (ITO) in developing transparent electronics, energy harvesting devices, and integrated sensors [25].

Growth methods for ZnO nanowires

Vapor–liquid–solid

Vapor–liquid–solid (VLS), also known as metal catalytic growth, is a mechanism for nanostructure growth, which

was first proposed by Wagner and Ellis in 1964 [26]. They managed to grow and synthesize crystalline silicon whiskers from vapor sources such as silicon tetrachloride ($SiCl_4$) and silane (SiH_4), using gold (Au) particles as a catalyst. In general, nanostructures grow in areas seeded by the metal catalyst. Therefore, their diameters are mainly determined by the size of the catalyst. In the case of nanowires, the VLS method uses nano-sized metal clusters as catalyst to absorb gas phase reactants and to form eutectic alloy drops—as the reactants in the droplets become supersaturated, precipitation takes over and one dimensional nanowires begin to form [24]. Figure 2 illustrates this process.

This technique usually involves growing ZnO nanowires on silicon (Si) or sapphire (Al_2O_3) substrates with the presence of a metal catalyst. Some popular catalysts include: Au, silver (Ag), platinum (Pt), copper (Cu), and tin (Sn) [27]. Typically, the ZnO nanowires are grown at temperatures above 600 °C with a pressure in the cylinder ranging between 3 and 30 Torr under a constant flow rate of 100–250 sccm of argon (Ar) gas [24, 28–31]. For example, in [28], Au was deposited over porous Si substrate by sputtering. The Au-enriched Si substrate was then placed on a quartz boat and put into the center of a quartz tube within a furnace. A 1:1 ratio of ZnO and graphite were used as starting materials in pressures between 5 and 30 Torr. The temperature of the furnace was then increased to 950 °C at a rate of 50 °C/min and high purity Ar gas was introduced to the quartz tube at a flow rate between 120 and 250 sccm.

Sparsely dispersed vertical ZnO nanowires with a preferred (002) orientation and high crystal quality using a self-catalyzed VLS method have also been achieved [24]. The process includes a deposition of a 50 nm thick electrically conductive gallium (Ga)-doped ZnO thin film onto a sapphire substrate by radio frequency magnetron sputtering. This deposition technique uses a combination of O_2 and Ar at flow rates of 54.4 and 0.8 sccm, respectively—with a temperature of 600 °C and pressure of 10 Torr for 20 min. The ZnO growth occurs in two phases. First, only Ar is introduced into the furnace at a flow rate of 54.4 sccm and the temperature is increased at a rate of 30 °C/min. The chamber pressure is kept at 10 Torr. When the temperature reaches 450 °C, O_2 is introduced at a flow rate of 0.8 sccm. At 600 °C the ramping process ends and the temperature is maintained to allow ZnO nanowire to grow. ZnO begins to form pyramid-like structures as the thickness of the ZnO film increases but since the ZnO film was oriented in the (002) direction, the growth rate of the ZnO nanowires along the *c* axis should exceed that of other prismatic sides and allows for sparsely dispersed vertical ZnO nanowires (Fig. 3). Inspection by X-ray diffraction (XRD) indicates an orientation in the (002) direction (Fig. 4).

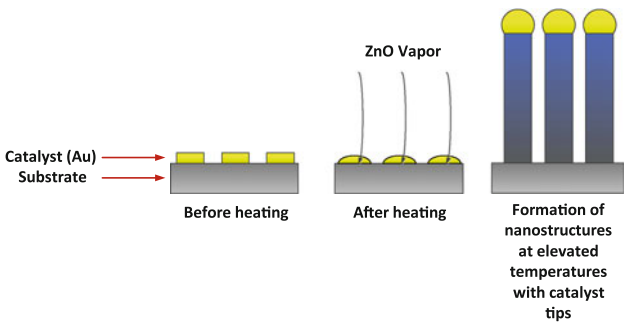

Fig. 2 Diagram of vapor–liquid–solid deposition. The Au catalyst forms eutectic alloy drops that become supersaturated allowing for ZnO nanowires to form

Another approached explored by Chang and co-workers [32] implements a vapor trapping mechanism to synthesize n-type ZnO nanowires with high carrier concentration without incorporating dopants. This method provides a controlled nanowire growth by creating spatial variations to allow donors to be directly introduced to the ZnO nanowires during the synthesis process. The synthesis is performed using a VLS growth mechanism in a quartz vial under a quartz tube in order to exploit native ZnO defects

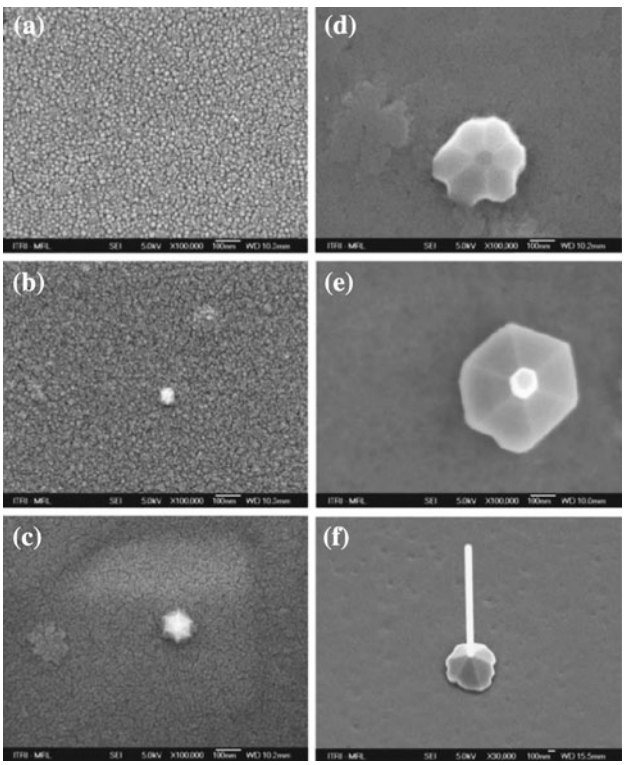

Fig. 3 Top-view SEM micrographs of **a** sputtered-ZnO:Ga films without ZnO nanowires, **b** single ZnO nanowire grown for 1.5 min, **c** single ZnO nanowire grown for 3 min, **d** single ZnO nanowire grown for 4.5 min, **e** single ZnO nanowire grown for 20 min., **f** 30°-tilted SEM micrographs of a single ZnO nanowire grown for 20 min (image courtesy of Dr. Eugene I-Cherng Chen)

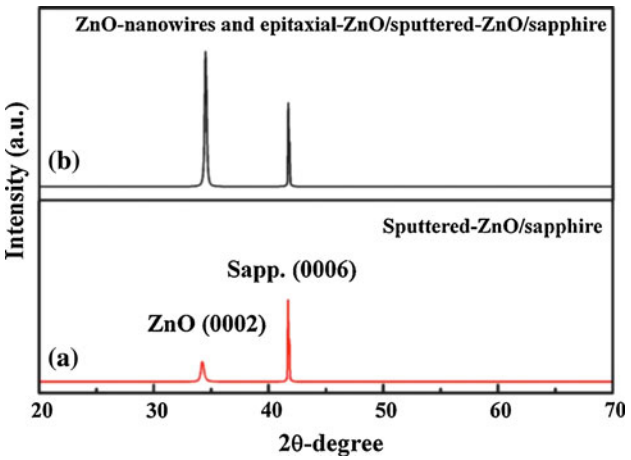

Fig. 4 Color online. XRD spectra measured at room temperature for (*a*) sputtered-ZnO:Ga/sapphire sample, and (*b*) ZnO nanowires and epitaxial-ZnO/sputtered-ZnO:Ga/sapphire sample (image courtesy of Dr. Eugene I-Cherng Chen)

such as zinc interstitials and oxygen vacancies to obtain a zinc-rich environment.

Physical properties of the ZnO nanowires such as the size and shape can be controlled by the thickness of the catalyst tip. Controlling the size of the catalyst particle can control the size of the ZnO nanowire [19]. Wang et al. [33] report on controlling the growth of ZnO nanowires by selecting different catalysts. Their findings suggest that Au catalyst growth results in the smallest diameter and longest length nanowires when compared to Pt and Ag.

As demonstrated by these variations of the VLS mechanism, it can be used to synthesize uniform structures of ZnO nanowires with relatively simple setup and control. It has very low activation energy when compared to physical vapor deposition. One major drawback of the VLS method is the unavoidable contamination due to the metal catalyst. Metal residue can have negative impact on the efficiency of radiative recombination processes and can also result in unidirectional growth [34].

Physical vapor deposition

Physical vapor deposition (PVD), also known as vapor–solid (VS), is a process in which the source material is sublimated into a vapor form at high temperatures, usually in a furnace, and then deposited onto a substrate at a lower temperature (see Fig. 5). There are several different PVD techniques, which use a variety of different reactive gasses to dissociate and ionize plasma. This in turn reacts with the target metal atoms. These techniques include electron beam physical vapor deposition (EBPVD), cathode arc physical vapor deposition (Arc-PVD), pulse laser deposition (PLD), and ion beam sputtering (IBS).

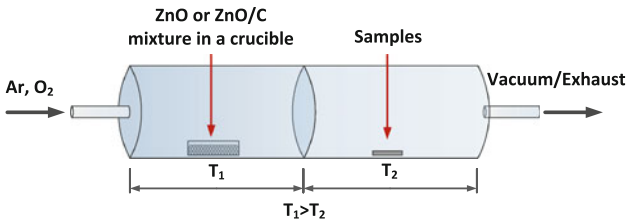

Fig. 5 Diagram of physical vapor deposition. The two-temperature zone furnace consist of high temperature zone where sublimation occurs and a low temperature zone where sublimated ZnO deposits onto the substrates. Ar is usually used as the carrier while O2 is used as the reactant gas

EBPVD is an evaporation PVD method, in which high-energy electron beam bombardments transform a source material into a vapor. The source material is then cooled, depositing onto the target material. EBPVD allows for localized heating of material and controlled evaporation rates. However, it cannot coat surfaces with complex geometries and the evaporation rate may result in non-uniformity. Arc-PVD, is another PVD evaporation approach, where the arc of very high direct current is used to interact with the source material. Like the EBPVD, the source material is cooled and deposited over the target material. Arc-PVD can be versatile depending on the target materials used but it produces microdroplets which can have adverse effects to uniformity [35]. Unlike EBPVD, PLD is a simple PVD technique capable of depositing on materials with complex geometries. It uses high power laser pulses to ablate the surface of the source material before depositing the plasma plume onto the heated substrate through nucleation. PLD is cost-effective and like Arc-PVD, it is versatile but produces microdroplets [35].

Sputtering PVD methods usually have a plasma or ion beam configuration. The deposition approach involves vaporizing atoms from the source material by bombarding them with energized particles. The energized particles kinetically knock atoms in the surface from their equilibrium states. The atoms then begin to travel into the target material and undergo further collisions. The process continues causing atoms to be ejected or sputtered from the target surface. IBS is a sputtering technique in which an ion beam is targeted onto the source material and the atoms are ejected to a nearby substrate. The biggest advantage of implementing this approach is that the sputtered atoms have a high average energy for deposition and the controlled ion bombardment results in significant nanostructural modification of properties. Nevertheless, cost can quickly become a factor depending on the size of the ion beam and the substrate [35].

Typically, the growth of ZnO nanowires has been achieved on silicon and sapphire substrates using PVD method. In general, Ar is used as a carrier gas [36],

however, O_2 has also been successfully used [37]. The carrier gas transports the vapor from the high temperature zone of the tube furnace to the low temperature zone. The substrate deposition temperature ranges from 150 to 550 °C, therefore greatly bordering the substrate selection range [35]. High purity zinc powders are placed in a quartz or alumina boat, which is inserted in a horizontal quartz or alumina tube furnace [27].

In general, in the PVD process, coating material is vaporized or sputtered in a chamber to produce a flux of atoms or molecules which condenses on the substrate to be coated [35]. The zinc oxide powder is sometimes vaporized in low-pressure conditions ranging from 0.074 to 0.200 Torr [38] because ZnO does not sublimate at 1000 °C in atmospheric conditions [33]. Another approach to decrease the temperature required to vaporize ZnO is mixing the powder with carbon. Fang et al. reports the influence of growth temperature on the morphology of ZnO nanowires grown at 930, 960, and 990 °C. An average diameter was 100 nm for ZnO nanowires grown at 930 and 990 °C. The ZnO nanowires grown at 960 °C had a bottom diameter of 400 nm and a top diameter of 200 nm. The ZnO nanowires had an average length of 15 μm when grown at a temperature of 930 °C and 5 μm when grown at 960 or 990 °C [39].

ZnO nanowires can be easily synthesized using PVD with or without the use of a catalyst. The catalyst approach usually involves Au. For example, in [40], zinc powder with purity >90 % was evaporated at a temperature of 400 °C and Si wafers with well dispersed Au nanoparticles were put 2 cm apart in the middle of a quartz tube inside a horizontal furnace. At 400 °C N_2/O_2 were introduced at a flow rate of 100/20 sccm, respectively, for 30 min. The system was then allowed to cool to room temperature under N_2, which allowed for uniform growth of ZnO nanowires with diameters of 10 nm and lengths of 10 μm.

While using catalysts allow for highly controlled growth, it is often beneficial to implement a PVD process without the use of a catalyst to eliminate any possible contamination or impurities. Multiple studies were carried out by Tigli and co-workers [27, 41] to determine the effects of various process parameters on the quality of the synthesized ZnO nanowires using PVD. Initially, the experiments were carried out with temperatures from 800 to 1200 °C. This produced ZnO nanowires with smooth surfaces and uniform diameters in the range of 50–120 nm and lengths of 2–7.1 μm without the use of any catalyst, thin-film deposition, or special pre-growth sample treatments. In the first experiment, approximately 1.38 g of zinc powder was placed in a quartz boat, which was then placed in a quartz tube inside a furnace. Si substrates were placed 5 cm apart downstream from the quartz boat. The procedure was achieved under a constant Ar flow rate of 400 sccm and chamber pressure of 63 Torr for 1 h. Varying temperatures were explored, with the high temperature zone ramped up to 828 °C when introducing Ar and then decreased at a rate of 5.76 °C/min to 473 °C when the Ar was turned off. The low temperature zone is maintained at 588 ± 2 °C [27]. This resulted in uncontrolled but uniform growth of ZnO nanowires along the Si substrates located at 2.5, 5, 10, and 15 cm from the quartz boat. The optimal distance for the best coverage of the Si substrate was determined to be 20 cm downstream from the quartz boat. However, limiting control over the furnace pressure due to the absence of the vacuum pump resulted in uncontrolled growth.

In another attempt, a three-temperature zone horizontal furnace was used with a gas-powered vacuum to achieve better control. In addition, A 1:1 mixture of graphite and ZnO powder was used to achieve a carbon-thermal reaction. The high temperature zone was ramped up to 1000 °C, while the second and third zone were kept at 750 and 650 °C, respectively. A continuous flow of Ar was introduced at 100 sccm, when the high temperature zone reached 1000 °C for 90 min. The pressure in the quartz tube was approximately 3.26 Torr throughout the entire process. Figure 6 shows the temperature readings throughout the second set of experiments. This procedure provided a larger temperature gradient between the high and low temperature zones and more importantly, allowed for a faster sublimation of nanoparticles. In both experiments, an accumulation of uniformly distributed ZnO nanowires appeared on the Si substrates. However, improved orientation was achieved using the 1:1 graphite to ZnO mixture in a controlled environment (Fig. 7). The end result of [41], showed that

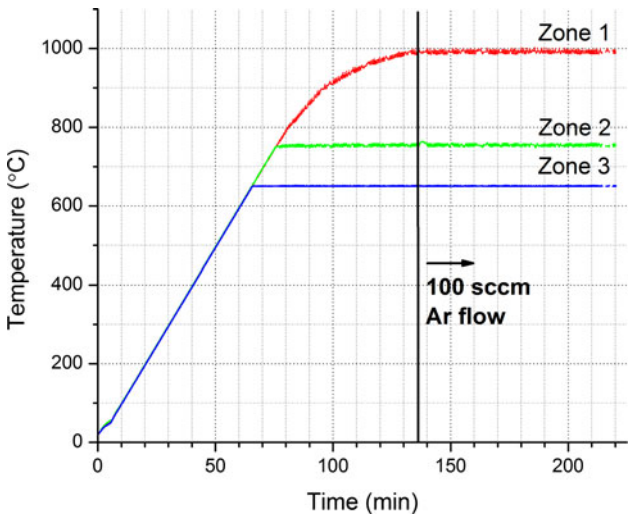

Fig. 6 Temperature readings for all active furnace zones throughout the set of experiments using a 1:1 mixture of graphite and ZnO powder (image courtesy of Dr. Onur Tigli)

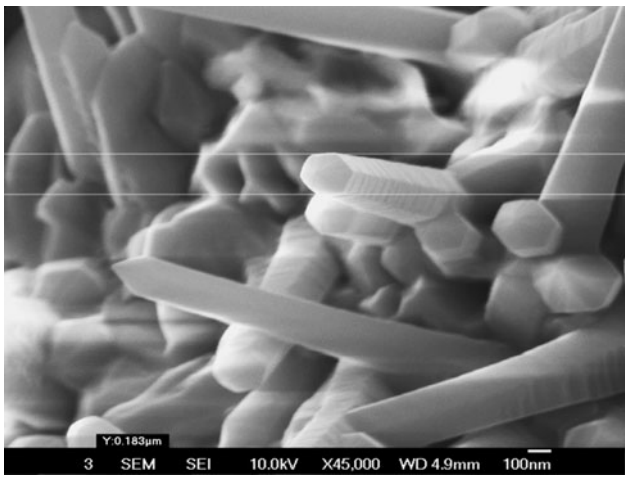

Fig. 7 SEM snapshot of synthesized ZnO nanowires. Diameter is approximately 183 nm (image courtesy of Dr. Onur Tigli)

this particular PVD approach offers a simple and inexpensive method to synthesize ZnO nanowires. Still, high temperatures were used and synthesizing at low temperature can decrease the stress between the ZnO nanowires and Si substrate [33].

Chemical vapor deposition

Chemical vapor deposition (CVD) is one of the most popular thin-film deposition technologies being employed due to its ability to provide uniform deposition over complex geometries. In the process, reduction or thermal decomposition decays chemical vapor precursor species. The material gets deposited on the surface when the vapor comes into contact with heated substrate surface [35]. The entire process can be broken down to five important steps. The first and second include diffusing the reactants to the substrate and adsorbing onto the surface. The third requires the surface chemical reactions to lead to a deposition of the solid. Then gaseous by-products begin a desorption process from the surface. Finally, gaseous by-products start to diffuse into the stream [35]. CVD is usually carried out at higher temperatures when compared to PVD and may contain corrosive by-products due to chemical reactions (see Fig. 8).

CVD covers a variety of reactor process types which are determined based on the material substrate, coating, morphology, uniformity, and cost. Some process types include atmospheric pressure chemical vapor deposition (APCVD), low-pressure chemical vapor deposition (LPCVD), and plasma-enhanced chemical vapor deposition (PECVD) [35]. APCVD offers a very high deposition rate but with low purity and poor uniformity. It operates in atmospheric conditions. LPCVD improves uniformity and purity but with higher temperatures and lower deposition rates than APCVD. PECVD on the other hand operates under low pressures but do not require thermal energy to accelerate the reaction process. By applying a radio frequency (RF), a glow discharge is produced, which transfers energy to the reactant gases. This allows for lower deposition temperature than APCVD and LPCVD [35].

Many different forms of CVD have been carried out in research, industry, and academia to grow ZnO nanowires. Kumar et al. [42] used a homemade vertical chemical vapor deposition reactor to study structural and optical properties of synthesized ZnO nanowires. Approximately 2 g of zinc powder was placed in an inner tube of a CVD reactor with a Si substrate coated with Ni or NiO placed vertically near it. The ZnO nanowire growth occurred at a reaction temperature of 500 °C with a pressure of 40 Torr under a 20 sccm flow of nitrogen gas and was later brought down to approximately 25 °C using H_2. This process resulted in high density needle-like structures when using NiO-coated Si substrates. The needle-like structures of ZnO had a top width of a 20 nm and bottom width of 300 nm. Most of the tips of the ZnO needle-like structures contained catalyst particles.

Doping ZnO has also been explored to add photoluminescence properties. For example, in [43] vertically aligned sulfur-doped ZnO nanowires were synthesized using CVD. In this process, Au was formed and used as a catalyst when Si substrates were coated with $HAuCl_4 \cdot 3H_2O$ in ethanol

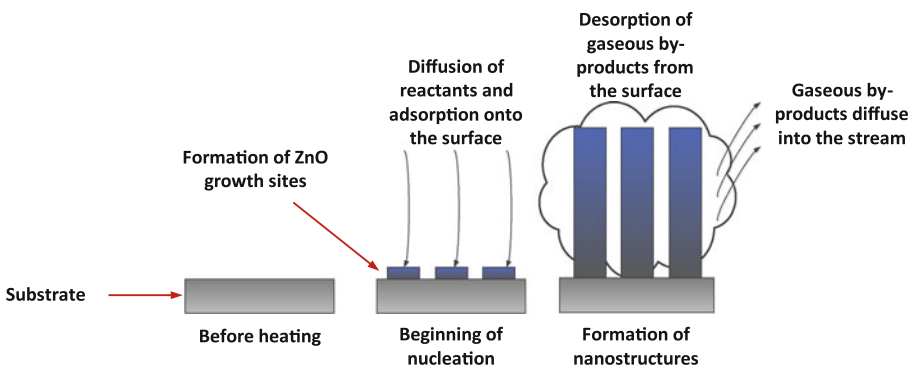

Fig. 8 Diagram of chemical vapor deposition. Consist of a five step process where diffusion, adsorption, deposition of the solid, desorption, and diffusion occurs on the surface of the substrate

solution. First, Si substrates containing zinc powder were positioned on quartz boat while sulfur powder was positioned at the entrance of the quartz tube. Then temperature of the CVD reactor was kept constant at 500 °C with Ar being introduced at a flow rate of 500 sccm for 2 h. This process produced 10–100 bundles of sulfur-doped ZnO nanowires with lengths of 10 μm and diameters of 20 nm. Transmission electron microscopy (TEM) revealed uniformity of sulfur-doped ZnO nanowires and that no amorphous phase or outer layer exists. Selected area electron diffraction (SAED) pattern confirmed that the nanowire consists of single crystalline ZnO with [001] direction. Like in VLS mechanism, the results proved that the size of the nanoparticle affects the diameter of the ZnO nanowire. The uniformity along the wire axis put forth the idea that pre-grown ZnO nanowires would be altered or even removed during the growth of the sulfur-doped ZnO nanowires. The diameter difference between the sulfur-doped ZnO nanowires and the regular ZnO shows that zinc, sulfur, and oxygen vapors deposit and form a liquid alloy on the nanosize surface of pre-grown ZnO nanowires. Thus, sulfur-doped ZnO nanowires' vertical alignment and the diameter are confined by the ZnO nanowires.

Metal–organic chemical vapor deposition

Metal–organic chemical vapor deposition (MOCVD) is a CVD technique implementing a metal–organic source gas (very weak bond) to be broken by thermal means. This allows for metal deposition while organic vapor is pumped away. For example, tantalum ethoxide ($Ta(OC_2H_5)_5$) is commonly used to create tantalum pentoxide (Ta_2O_5) and tetradimethylamino titanium (TDMAT) is used to create titanium nitride (TiN). Similar to other CVD techniques, MOCVD releases corrosive by-products and unused precursor species. Moreover, safety precautions must be taken when dealing with MOCVD as it may release organic by-products into the atmosphere. This can be dangerous as the human body has an affinity to absorb organic compounds with relative ease. These organic by-products can poison the body when their bonds break, leaving behind heavy metals that the human body cannot expel [35]. However, the growth of highly oriented arrays of ZnO nanostructure can be achieved using the MOCVD method. Still, this method is limited in mass production.

ZnO nanowires have been grown using both Si and sapphire substrates by the MOCVD method. Lee and coworkers [44] have reported growing catalyst-free ZnO nanowires using diethylzinc (DEZn) as a zinc precursor, O_2 as an oxidizer, and N_2 as a suppressor. Gallium arsenide (GaAs) substrates were used to grow collections of ZnO nanowires in a vertical flow reactor. Ar is introduced as a carrier gas circulated by a bubbling cylinder with the temperature of the DEZn cylinder kept at -0.15 °C. The substrate is placed in a quartz tube with a pressure of 15 Torr and temperature 599.85 °C [44, 45]. ZnO nanowires managed to grow when the vertical reactor was set to a pressure of 15 and 24.98 Torr. When the reaction chamber was maintained at 24.98 Torr the nanowire diameter was 300 nm with a length of 3.775 μm. At a pressure of 15 Torr, the diameter and length of the nanowire were 100.0 and 774.5 nm, respectively [44]. Lee et al. also reports on the growth of ZnO nanowires using both the MOCVD method and the thermal evaporation method. However, ZnO nanowires grown by the PVD method had an average diameter of 100 nm and an average length of 3 μm.

ZnO nanowire growth using other substrates with similar crystal lattice structure and band gaps has also been achieved. These include gallium nitride (GaN), aluminum nitride (AlN), and epilayers of aluminum gallium nitride ($Al_{0.5}Ga_{0.5}N$). This approach can be beneficial in order to produce heterostructure devices and make electronic measurements. In [46], a combinational deposition method which engaged both MOCVD and VLS was implemented. Using the MOCVD technique and a gold catalyst, thicknesses between 2 μm and 500 nm of GaN and AlN thin films and 205 nm thick $Al_{0.5}Ga_{0.5}N$ film, were grown on a- and c-plane sapphire substrates, respectively. A mixture of 0.6 g each of ZnO and graphite powder was loaded to a single-zone furnace. A combination of Ar and O_2 was used as a carrier gas with a flow rate of 49 and 1 sccm, respectively. The temperature of the furnace was increased at a rate of 50 °C/min until the temperature reached 950 °C. This temperature was maintained and the pressure of the chamber was kept at 22.502 Torr for 30 min. This heated the source material. However, the local temperature of the substrates was 880 °C. The furnace was then turned off and let cool to room temperature for 2 h under Ar [46].

This combinational approach of MOCVD and VLS produces ZnO nanowires with uniform diameter perpendicular to the substrate. Measurements taken using TEM shows that the GaN had an average length of 434 nm and an average diameter of 28 ± 6 nm. ZnO nanowires grown on the AlN substrates had longer average lengths of 500 nm and diameters of 22 ± 2 nm (Fig. 9). XRD analysis showed that ZnO nanowires were aligned for all three substrates used. A diffraction of (0002) and (0004) at 34.63° and 72.76°, respectively, were detected in the atomic plane of ZnO in all three spectra. The GaN plane of (0002) overlapped that of ZnO while the peaks of AlN and $Al_{0.5}Ga_{0.5}N$ were gradually separated due to having a larger lattice mismatch (Fig. 10). This method showed that even when implementing a non-catalyst MOCVD technique, it lacks control over the growth position. Therefore, combining it with the VLS process can precisely control

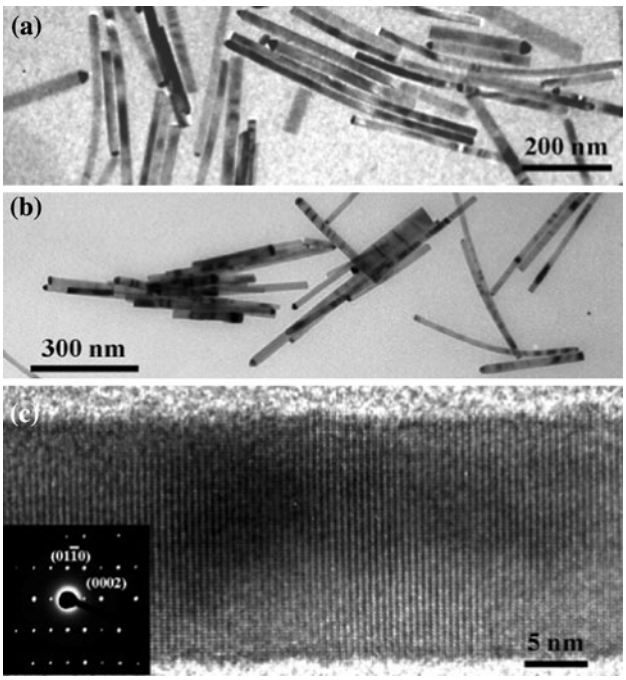

Fig. 9 Low-magnification TEM image of ZnO nanorods grown on GaN (**a**) and AlN (**b**) substrates. **c** High-magnification TEM image of a single ZnO nanorod; (*inset*) the corresponding electron diffraction pattern of the ZnO nanorod shown in (**c**) (image courtesy of Dr. Zhong Lin Wang)

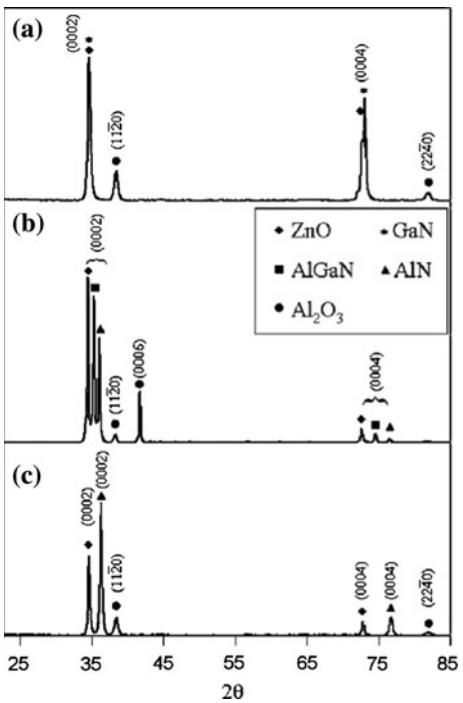

Fig. 10 XRD spectra of aligned ZnO nanorods growing on GaN (*a*), Al0.5Ga0.5N (*b*), and AlN (*c*) substrates (image courtesy of Dr. Zhong Lin Wang)

the position and aligned the ZnO nanowires by patterning it with a gold catalyst [46]. In [46], method gives rise to the possibility of growing vertically aligned heterojunction devices with tunable optical properties at the nanoscale using a combination of MOCVD and VLS growth methods.

Hydrothermal-based chemical approach

The hydrothermal-based chemical approach is a simple, low cost, low temperature method that can result in high volume production of ZnO nanostructures. However, this process may result in poor crystal quality, especially in aqueous solutions. Solution-based methods often utilize templates, which contain channels to act as a structural director for the nanostructure. The templates are categorized as soft or hard templates, such as anodic alumina membranes (AAM) [47].

As reported by Greene et al., the surface of the substrate is coated with crystal seeds (dodecanethiol-stabilized Au nanocrystals, ZnO nanocrystals, etc.). To establish adhesion, the substrate is annealed between coatings [47]. The substrate is then placed upside down in an aqueous solution to allow the ZnO nanowires to grow [47]. Zhang and co-workers [48] performed a microemulsion-mediated hydrothermal process for ZnO nanowire growth. Their reaction media consisted of 1 g of cetyltrimethylammonium bromide (CTAB), 1.2 mL of tetrahydroxozincate $Zn(OH)_4^{2-}$, 3 mL of *n*-hexanol, and 10.2 mL of *n*-heptane for the microemulsion. Continuous stirring was necessary before the microemulsion was transferred to a 25 mL Teflon-lined autoclave. This was then heated at a temperature of 140 °C for 13 h. This formed a white precipice, which was washed repeatedly with ethanol and distilled water. After centrifugation and drying in a vacuum at temperatures of 60–70 °C, a 21 % yield of ZnO nanowires were obtained.

Specific structural and optical properties can be obtained by doping ZnO nanowires during a hydrothermal chemical approach. Bai et al. [49] proposed a two-step process for synthesizing uniform and vertically aligned ZnO nanowires on Si substrates by doping with Al. The first step involves, preparing the Al-doped ZnO nanowires growth with a radio frequency (RF) sputtering magnetron to create a seeding layer on the substrate. The second step involves hydrothermal-based chemical deposition to allow Al-doped ZnO nanowire growth. Their process was seed-assisted. An 850 nm n-type thin film was deposited on p-type Si substrate via thermal evaporation. This allowed Al-doped ZnO nanowires to grow on a 40 nm thick seeding layer by RF magnetron sputtering and in situ annealing at a temperature of 550 °C for 3 h. The Al-doped Si substrate was then placed in a sealed container of 99.9 % pure aqueous solutions of both zinc nitrate hexahydrate ($Zn(NO_3)_2{\cdot}6H_2O$) and hexamethylenetetramine ($(CH_2)_6N_4$) at a temperature of

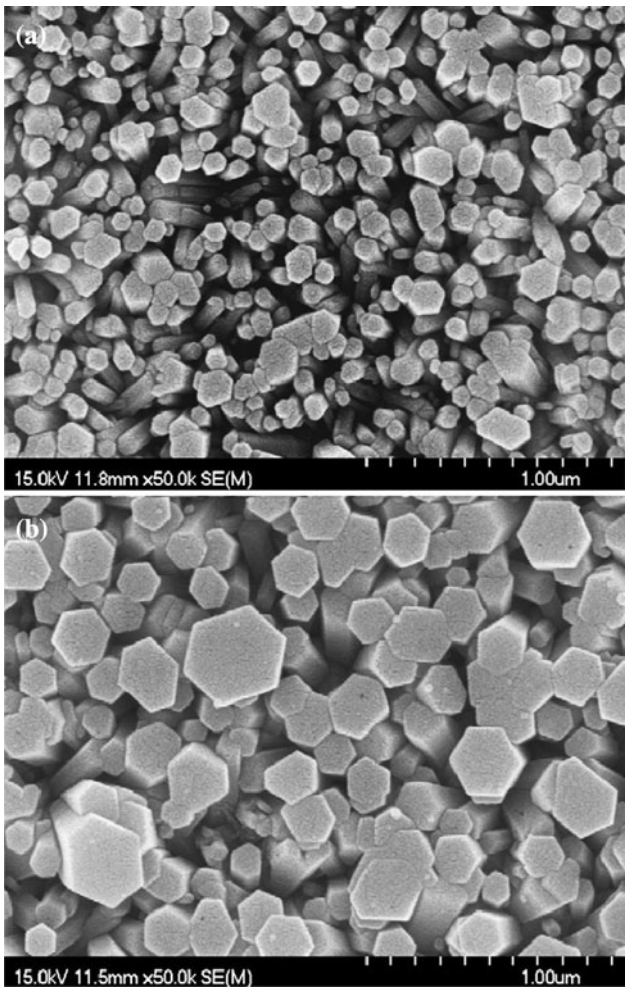

Fig. 11 SEM images of Al-doped ZnO nanowires annealed in the oxygen atmosphere at 550 °C for **a** 1 h **b** 7 h (image courtesy of Dr. Tseung-Yuen Tseng)

95 °C for 3 h. A thermal diffusion method at a temperature of 550–650 °C for 1–7 h was implemented to diffuse the Al from the thin-film layer and onto the ZnO nanowires under an oxygen atmosphere [49].

Field emission scanning electron microscopy (FESEM) results show smooth vertically aligned Al-doped ZnO nanowires with hexagonal structures (Fig. 11). The Al-doped ZnO nanowires had diameters of 80–210 nm. Their results indicated that the average diameter and the Al-doped ZnO nanowire collections increase as the growth time increases.

Other nanostructures

Gleiter [50] arranged the first nanostructure classification attempt using their crystalline forms and chemical composition as the basis for classes. However, this classification scheme proved to be incomplete as it neglected 0D and 1D structures such as nanoparticles and nanotubes, respectively. Therefore, a dimensionality classification scheme has been adopted to account for these missing structures [51–53]. In its simplest form, nanostructures are now categorized into four basic classes, 0D (i.e., nanoclusters and nanoparticles), 1D (i.e., nanotube and nanowires), 2D (i.e., nanoplates and layers), and 3D (i.e., nanotetrapods). The deposition method has a profound impact on morphology and can be engineered to fabricate novel structures.

The most popular approach for ZnO nanostructure growth are vapor transport methods utilizing Zn or ZnO powder mixtures in which they react with O_2 vapor to form nanostructures [54]. These vapor transport methods do not involve the use of a catalyst for growth and are performed in a vapor–solid approach. It has been documented that using different ratios and mixtures of Zn and ZnO powders in the presence of O_2 under different growth temperatures, changes morphology and allows the formation of novel nanostructures [32, 55]. Nanobelts, which can be described as a 2D nanowire with well-defined walls, are typically grown using a combination of 99.99 % ZnO powder and steady flow of O_2 under the PVD process. This is due to the composition of the oxide nanobelts resembling the original oxide source material synthesized [56–58].

Many tubular structures, such as the hexagonal tubular nanostructure, are said to first start off as ZnO nanorods before transforming to their respective shapes. This is due to oxidation occurring on the surface forming ZnO shells; then, when sublimation occurs, the core becomes hollow [59]. More exotic structures such as ZnO nanopropellers start off in a similar fashion. However, they are synthesized by modifying the composition of the source material, local temperature, and diffusion rate. Powder mixtures of ZnO and SnO_2 in a 1:1 ratio have been explored [61]. This resulted in a uniform growth because the Sn droplets have minimal effect on the diameter of the nanowire. Ultimately, the nanoblades form along the *a* axis <20>, which is perpendicular to the nanowire.

Mesoporous nanostructures follow a similar protocol as well. They are formed from Zn polyhedron synthesized during the first phase of PVD process. Oxidation of the Zn polyhedron forms the porous ZnO nanoshell previously described. Among the different types of mesoporous nanostructures are nanocages and nanoshells [62]. A composition of two parts ZnO and one part SnO_2 and graphite powder each were used as the source material to achieve these nanostructures. Figure 12 displays some novel ZnO nanostructures.

To summarize, morphology is highly dependent on three parameters: source material composition, growth temperatures, and diffusion rates. They are alike in that they are

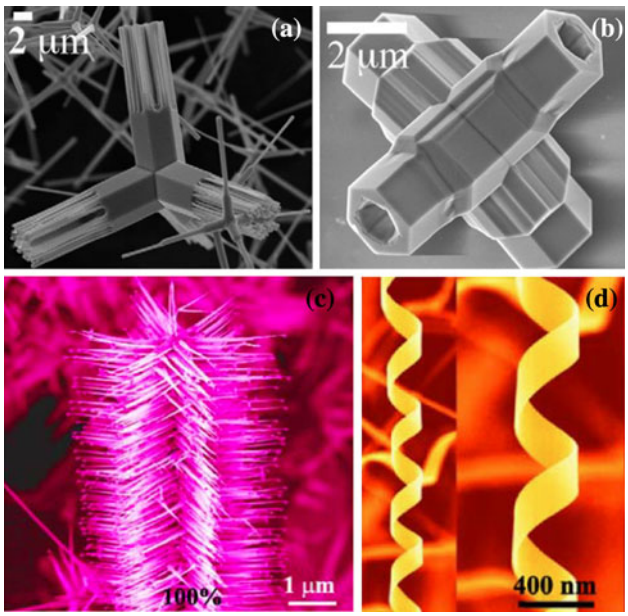

Fig. 12 SEM images of different ZnO nanostructure morphologies. **a**, **b** Nanotetrapods (image a and b courtesy of Dr. Aleksandra Djurišić). **c** Mesopourous nanowires, **d** nanospring (image c and d courtesy of Dr. Zhong Lin Wang)

fabricated using the vapor transport method, usually PVD, without the presence of a catalyst. The more complex structures that have been studied originate from simpler 0D and 1D nanostructures in which the diffusion rate greatly impacted morphology. However, applications for these exotic structures are sparse in comparison with more conservative 0D and 1D nanostructures such as nanoparticles and nanowires.

Applications

Zinc oxide nanostructures have a vast amount of potential applications encompassing several fields. The predominant ones include biosensing and optoelectronics. However, applications in energy storage and even hydrogen storage material have also been investigated [18]. New applications in the medical field are also attracting growing interest as the methods of ZnO nanostructures are getting more optimized for specific applications. As demonstrated by the maturity of the most prominently used methods reviewed in the previous section, it is a widely accepted notion that fabrication toolsets for obtaining ZnO nanostructures with designed physical qualities and chemical formations are readily well-developed and studied. Therefore, collective scientific research interest in this field is expected to gradually shift toward actual device fabrication using these nanostructures at their core. This shift will be primarily driven by applications with well-defined requirements and characteristics. In this section, we will evaluate the leading applications and summarize the potential growth prospects in similar fields.

Biosensors

The field of nanofabrication has been greatly supplemented by the medical industry and many applications have been tailored to diagnose and treat diseases. ZnO biosensors have been studied and fabricated, in part due to the possibility in improving detection sensitivity while offering a noninvasive approach for medical treatment. ZnO nanowires and nanotubes have been used to detect biological molecules in aqueous solutions. Popular ones include pH sensors, glucose biosensors, and cholesterol biosensors [18]. For instance, under 0.2 mM, ZnO nanocombs were successful in detecting glucose with a high sensitivity of 15.33 μA/cm^2 mM [63]. In this example, ZnO nanocombs were synthesized via the vapor transport method using 99.9 % ZnO powder on a Si substrate. After deposition, the Si substrate was transferred to a standard Au electrode commonly used in electrochemistry. The now ZnO/Au electrode was then briefly dipped in a 0.01 M PBS solution with a pH level of 7.4. After evaporation, 5 μl of GO_x ($\sim$40U/mg) and Nafion solution were applied to the surface of the ZnO/Au electrode. It was then stored in 4° C for 24 h to form a film. A three-electrode configuration was used to detect glucose in an electrochemical workstation (Bio-logic SA VMP2) [63].

ZnO nanoflowers have also been used to detect cholesterol oxidase (ChO_x) binding with a high sensitivity of 61.7 μA/cm^2 μM. This biosensor is important because cholesterol serum has been associated with many clinical disorder including coronary artery disease, cerebral thrombosis, and hypertension. The nanoflower structure was fabricated by combining hexagonal-shaped ZnO nanorods. This was then coated onto the surface of a 3.0 mm^2 Au electrode. Using a physical absorption technique, the ChO_x was fixed to the surface of the ZnO nanoflower. A thin film was formed on the surface of the ZnO nanoflower by applying 10 μL Nafion solution and letting it settle overnight at 4° C. Electrochemical experiments were then performed using an electrochemical analyzer [64].

Optoelectronics

Over the past decade, substantial improvements in ZnO's properties have been made. Some improvements include the tunability of its photoluminescence emission band from blue to yellow [65], the increased quantum yield of up to 85 % [66], and the stability of its nanoparticles in aqueous solution for biological labeling [67]. These improvements coupled with the fact that ZnO offers an affordable

non-toxic alternative to other photoluminescence semiconductor, have paved the way for its applications in optoelectronics. Different ZnO nanostructures have been created from hexagonal patterned nanorods [68] to nanopropellers [59]. However, 1D ZnO nanostructures such as nanowires, nanorods, and nanoribbons are the most commonly used when dealing with optoelectronics [60].

Popular applications in optoelectronics include light emitting diodes (LEDs), laser diodes, photodetectors, and photovoltaic cells. It has been shown that different deposition techniques can alter the optical spectrum [69]. Therefore, different deposition methods have been explored to synthesize 1D nanostructures for optoelectronic use. Green emissions occur when ZnO nanowires are fabricated by thermal evaporation methods [69], while solution based depositions exhibit yellow-orange emissions and in some cases blue [70]. For example, in [71], the MOCVD technique is implemented to grow vertically aligned ZnO nanorods/nanotips on transparent GaN blue LED electrodes. Kim et al. suggest that the output power of GaN blue LEDs with ZnO nanorod/nanotip arrays can improve ordinary GaN blue LEDs by up to 57 % at 20 mA.

ZnO laser diodes have been approached in two different fashions—amplified spontaneous emission and electrically pumped lasing. An example of the former involves using a simple vapor transport and condensation process where <0001> oriented ZnO nanowires arrays are synthesized on sapphire substrates. This method forms natural cavities with diameters ranging between 20 and 150 nm and lengths up to 10 μm. These cavities serve as shell for miniaturized laser diodes that can be used for optical computing, information storage, and microanalysis [72].

Conclusion and outlook

Zinc oxide nanostructure's future is dependent on the improvements in its biosensing and optoelectronics

Table 1 Summary of advantages and disadvantages for the different deposition techniques reviewed

Deposition technique	Advantages	Disadvantages
Vapor–liquid–solid (VLS)	Low activation energy	Contamination due to metal catalyst
	Simple setup	Unidirectional growth
	Controlled growth	
General physical vapor deposition (Furnace)	Simple setup	Temperature gradient limitation due to furnace
	Cost efficient	
Electron beam physical vapor deposition (EBPVD)	Controlled evaporation rates	Cannot coat complex geometries
		May result in non-uniformity
Cathode Arc physical vapor deposition (Arc-PVD)	Versatile	Produces micro-droplets which can affect uniformity
	High deposition rates	
Pulse laser deposition (PLD)	Ease of use	Splashing may result in macro/microdroplets
	Cost-effective	
	Versatile	
Ion beam sputtering (IBS)	Significant micro/nanostructural modifications	Expensive
		Tendency to introduce impurities because of lesser vacuum ranges
	High average energy for deposition	
Atmospheric pressure chemical vapor deposition (APCVD)	Ease of use	Low purity
	High deposition rate	Poor uniformity
Low-pressure chemical vapor deposition (LPCVD)	Excellent purity	Low deposition rates
	Excellent uniformity	Requires higher temperatures than APCVD
Plasma-enhanced chemical vapor deposition (PECVD)	Lower temperature than APCVD and LPCVD	Expensive
		Slow growth times
	Operates under low pressures	
Metal–organic chemical vapor deposition (MOCVD)	Excellent uniformity	Releases corrosive by-products
	Excellent growth orientation	Higher safety measures required due to toxicity
		Limited in mass production
Hydrothermal-based chemical approach	Ease of use	Poor crystal quality
	Low cost	
	Low temperature	
	High yield	

applications. It is possible that the focus shift toward carbon-based materials and the inability to accomplish p-type doping in a reproducible way may be hindering its growth in recent years. However, innovative experiments using different, more exotic nanostructures have shown great potential in biosensing and optoelectronics applications and may contribute to another revival.

Knowledge and advances in deposition techniques have played a pivotal role in exploring different ZnO nanostructure morphology as we saw in the case of ZnO nanoflower cholesterol biosensor. By combining simpler 0D and 1D nanostructures, more complex 2D and 3D nanostructures can be formed and their benefits exploited. Nevertheless, a thorough analysis of different deposition techniques is necessary to gain a foundation and understanding of ZnO nanostructure growth. Their advantages and disadvantages need to be examined and evaluated carefully to determine the correct protocol to achieve maximum yield that is suitable for application. The table below summarizes the respective advantages and disadvantages that were previously discussed in Table 1.

Application purpose often dictates the choice of the deposition method. In the case of VLS, contamination due to the presence of a metal catalyst is usually regarded as a negative side effect. However, this approach may be beneficial if the goal is to obtain metal contacts. Controlled growth is also possible as Wang et al. reported the direct relationship between the metal catalyst and the size/shape of the ZnO nanowires. By the same token, this may result in unidirectional vertical growth, which may not be practical for some biosensing applications.

PVD offers many different approaches to sublimate the source material into a vapor form. Among them you have: EBPVD, Arc-PVD, PLD, and IBS. A particular PVD method should be selected based on geometry complexity and cost. For example, Arc-PVD and PLD are capable of coating complex geometries as oppose to EBPVD. Moreover, IBS offers the ability of modifying nanostructural properties, making it tunable for different applications, but it comes at a high cost. A system of checks and balances exist when deciding on a particular PVD technique.

Like PVD, CVD offers a variety of different techniques including: APCVD, LPCVD, PECVD, and MOCVD. Unlike PVD, the CVD process requires a more challenging setup since chemical reaction plays a pivotal role in ZnO nanostructure growth. Nonetheless, high purity and uniformity can be achieved through LPCVD and MOCVD. The rule of thumb in the CVD process is that the quicker and simpler the technique, the lower purity and uniformity achieved.

The hydrothermal-based chemical approach is one of the more obscure methods for ZnO nanostructure growth. However, it offers several advantages such as low cost, temperature, and high yield. Its downside is poor resulting crystal quality, which at times can make applications in biosensing unpredictable. In the end, the most popular deposition methods for ZnO nanostructure growth were presented in this review and have been tested to be superior growth methods when compared to others. ZnO nanostructure fate is dependent on the discovery of new and innovative applications. Although the trend has begun to slow down, ZnO nanostructure research is still developing proving that this topic is still in its infant stages.

Acknowledgements We would like to thank the Departments of Electrical & Computer Engineering and Pathology as well as the Dr. John T. Mcdonald Biomedical Nanotechnology Institute, Miller School of Medicine, at the University of Miami. We would also like to thank our fellow colleagues for sharing their advice and knowledge—in particular, Sukru Ufuk Senveli from the University of Miami in Coral Gables, Florida, USA.

References

1. Brubaker DG, Fuller ML (1945) J Appl Phys 16:128
2. Klingshirn C, Hauschild R, Priller H, Zeller J, Decker M, Kalt H (2006) Adv Spectrosc Lasers Sens 231:277
3. Leung V, Ko F (2011) Polym Adv Technol 22:350
4. Nambiar S, Yeow JTW (2011) Biosens Bioelectron 26:1825
5. Castro Neto AH, Guinea F, Peres NMR, Novoselov KS, Geim AK (2009) Rev Modern Phys 81:109
6. Chen XM, Wu GH, Jiang YQ, Wang YR, Chen X (2011) Analyst 136:4631
7. Artiles MS, Rout CS, Fisher TS (2011) Adv Drug Deliv Rev 63:1352
8. Geim AK (2011) Rev Mod Phys 83:851
9. Cao BQ, Teng XM, Heo SH, Li Y, Cho SO, Li GH, Cai WP (2007) J Phys Chem C 111:2470
10. Fryar J, McGlynn E, Henry MO, Cafolla AA, Hanson CJ (2004) Nanotechnology 15:1797
11. Shen GZ, Chen D, Lee CJ (2006) J Phys Chem B 110:15689
12. Calestani D, Zha MZ, Zanotti L, Villani M, Zappettini A (2011) CrystEngComm 13:1707
13. Hsu YK, Lin YG, Chen YC (2011) Electrochem Commun 13:1383
14. Zhang P, Xu F, Navrotsky A, Lee JS, Kim ST, Liu J (2007) Chem Mater 19:5687
15. Liu WC, Cai W (2008) J Cryst Growth 310:843
16. Jimenez-Cadena G, Comini E, Ferroni M, Vomiero A, Sberveglieri G (2010) Mater Chem Phys 124:694
17. Wang J, Zhuang HZ, Li JL, Xu P (2011) Appl Surf Sci 257:2097
18. Ahmad M, Zhu J (2011) J Mater Chem 21:599
19. Wang ZL, Gao PX (2004) J Phys Chem B 108:7534
20. Gomez JL, Tigli O (2011) In: IEEE NMDC, Jeju
21. Carcia PF, McLean RS, Reilly MH, Crawford MK, Blanchard EN, Kattamis AZ, Wagner S (2007) J Appl Phys 102: 074512
22. Ozgur U, Alivov YI, Liu C, Teke A, Reshchikov MA, Dogan S, Avrutin V, Cho SJ, Morkoc H (2005) J Appl Phys 98: 041301
23. Klingshirn C, Fallert J, Zhou H, Sartor J, Thiele C, Maier-Flaig F, Schneider D, Kalt H (2010) Phys Status Solid B-Basic Solid State Phys 247:1424
24. Hsueh TJ, Hsu CL, Chang SJ, Lin YR, Lin TS, Chen IC (2007) J Electrochem Soc 154:H153
25. Hahn YB (2011) Korean J Chem Eng 28:1797

26. Wagner RS, Ellis WC (1964) Appl Phys Lett 4:89
27. Tigli O, Juhala J (2011) In: IEEE Nanotechnology, Portland
28. Hsu HC, Cheng CS, Chang CC, Yang S, Chang CS, Hsieh WF (2005) Nanotechnology 16:297
29. Snyder RL, Kirkham M, Wang XD, Wang ZL (2007) Nanotechnology 18: 365304
30. Chen IC, Hsueh TJ, Hsu CL, Chang SJ (2007) Sensors Actuators B-Chem 126:473
31. Yang PD, Huang MH, Wu YY, Feick H, Tran N, Weber E (2001) Adv Mater 13:113
32. Lu JG, Chang PC, Fan ZY, Wang DW, Tseng WY, Chiou WA, Hong J (2004) Chem Mater 16:5133
33. Wang N, Cai Y, Zhang RQ (2008) Mater Sci Eng R-Rep 60:1
34. Sallet V, Agouram S, Falyouni F, Marzouki A, Haneche N, Sartel C, Lusson A, Enouz-Vedrenne S, Munoz-Sanjose V, Galtier P (2010) Phys Status Solidi B-Basic Solid State Phys 247:1683
35. Hornyak GL (2009) Fundamentals of nanotechnology. CRC Press, Boca Raton
36. Yu DP, Zhang Y, Jia HB, Wang RM, Chen CP, Luo XH, Lee CJ (2003) Appl Phys Lett 83:4631
37. Zhang X, Wang LS, Zhou GY (2005) Rev Adv Mater Sci 10:69
38. Zhang XZ, Wang LS, Zhao SQ, Zhou GY, Zhou YL, Qi JJ (2005) Appl Phys Lett 86:231903
39. Zhao DX, Fang F, Zhang JY, Shen DZ, Lu YM, Fan XW, Li BH, Wang XH (2008) Mater Lett 62:1092
40. Zhang J, Wang X, Li QQ, Liu ZB, Liu ZF, Wang RM (2004) Appl Phys Lett 84:4941
41. Gomez JL, Senveli SU, Tigli O (2012) In: Miami 2012 winter symposium: nanotechnology in biomedicine, Miami, p P18
42. Kumar MS, Kim TY, Kim JY, Suh EK, Nahm KS (2004) In: Proceedings of 5th international symposium on blue laser and light emitting diodes, p 2554
43. Park JH, Bae SY, Seo HW (2004) J Phys Chem B 108:5206
44. Myoung JM, Lee W, Jeong MC (2004) Acta Mater 52:3949
45. Lee WN, Jeong MC, Myoung JM (2004) Nanotechnology 15:254
46. Wang ZL, Wang XD, Song JH, Li P, Ryou JH, Dupuis RD, Summers CJ (2005) J Am Chem Soc 127:7920
47. Yang PD, Greene LE, Law M, Tan DH, Montano M, Goldberger J, Somorjai G (2005) Nano Lett 5:1231
48. Yan CH, Zhang J, Sun LD, Pan HY, Liao CS (2002) New J Chem 26:33
49. Bai SN, Tsai HH, Tseng TY (2007) Thin Solid Films 516:155
50. Gleiter H (2000) Acta Mater 48:1
51. Pokropivny VV, Skorokhod VV (2007) Mater Sci Eng C-Biomimetic Supramol Syst 27:990
52. Kustov E, Nefedov V (2008) Russ J Inorg Chem 53:2103
53. Kustov EF, Nefedov VI (2007) Dokl Phys Chem 414:150
54. Fan ZY, Lu JG (2005) J Nanosci Nanotechnol 5:1561
55. Tian Y, Lu HB, Wu Y, Li JC (2010) Mater Sci Technol 26:1248
56. Sears GW (1955) Acta Metall 3:367
57. Pan ZW, Dai ZR, Wang ZL (2001) Science 291:1947
58. Yang PD, Lieber CM (1997) J Mater Res 12:2981
59. Wang ZL (2007) Appl Phys A-Mater Sci Proc 88:7
60. Djurisic AB, Ng AMC, Chen XY (2010) Prog Quantum Electron 34:191
61. Gao PX, Wang ZL (2004) Appl Phys Lett 84:2883
62. Gao PX, Wang ZL (2003) J Am Chem Soc 125:11299
63. Wang JX, Sun XW, Wei A, Lei Y, Cai XP, Li CM, Dong ZL (2006) Appl Phys Lett 88: 233106
64. Umar A, Rahman MM, Al-Hajry A, Hahn YB (2009) Talanta 78:284
65. Xiong HM, Liu DP, Xia YY, Chen JS (2005) Chem Mater 17:3062
66. Xiong HM, Wang ZD, Xia YY (2006) Adv Mater 18:748+
67. Xiong HM, Xu Y, Ren OG, Xia YY (2008) J Am Chem Soc 130:7522+
68. Wang XD, Summers CJ, Wang ZL (2004) Nano Lett 4:423
69. Hosono H (2004) Int J Appl Ceram Technol 1:106
70. Hosono H (2004) In: Critical interfacial issues in thin-film optoelectronic and energy conversion devices, vol. 796. MRS proceedings, p. 87
71. Kim KK, Lee SD, Kim H, Park JC, Lee SN, Park Y, Park SJ, Kim SW (2009) Appl Phys Lett 94:071118
72. Huang MH, Mao S, Feick H, Yan HQ, Wu YY, Kind H, Weber E, Russo R, Yang PD (2001) Science 292:1897